AGU PUBLICATIONS

Geophysical Research letters

Supporting Information for

Global monitoring data shows grain size controls turbidity current structure

D. Vendettuoli[1-2], M. A. Clare[1], E.J. Sumner[2], M.J.B. Cartigny[3], P.J. Talling[3], J. Wood[4], L.P. Bailey[1-2], M. Azpiroz - Zabala[5], C.K. Paull[6], R. Gwiazda[6], J.P. Xu[7], C. Stacey[8], D.G. Lintern[8], S.M. Simmons[9], E.L Pope[3] and S. Hage[10]

[1] National Oceanography Centre, University of Southampton, Waterfront campus, Southampton SO14 3ZH, UK

[2] School of Ocean and Earth Science, University of Southampton, Southampton, SO14 3ZH, UK

[3] Department of Earth Sciences and Geography, Durham University, Durham DH1 3LE, UK

[4] Ocean Data Technologies, Inc., 31 School Street Hyannis, MA 02601

[5] Faculty of Civil Engineering and Geoscience, Delft University of Technology, 2628 CN Delft, The Netherlands

[6] Monterey Bay Aquarium Research Institute (MBARI), 7700 Sandholdt Rd, Moss Landing, CA 95039, USA

[7] Southern University of Science and Technology, Shenzhen, China

[8] Geological Survey of Canada, Institute of Ocean Science, Canada

[9] Energy and Environment Institute, University of Hull, Hull, HU6 7RX, U.K.

[10] Department of Geoscience, Calgary University, AB Canada

Contents of this file

Additional Supporting Information

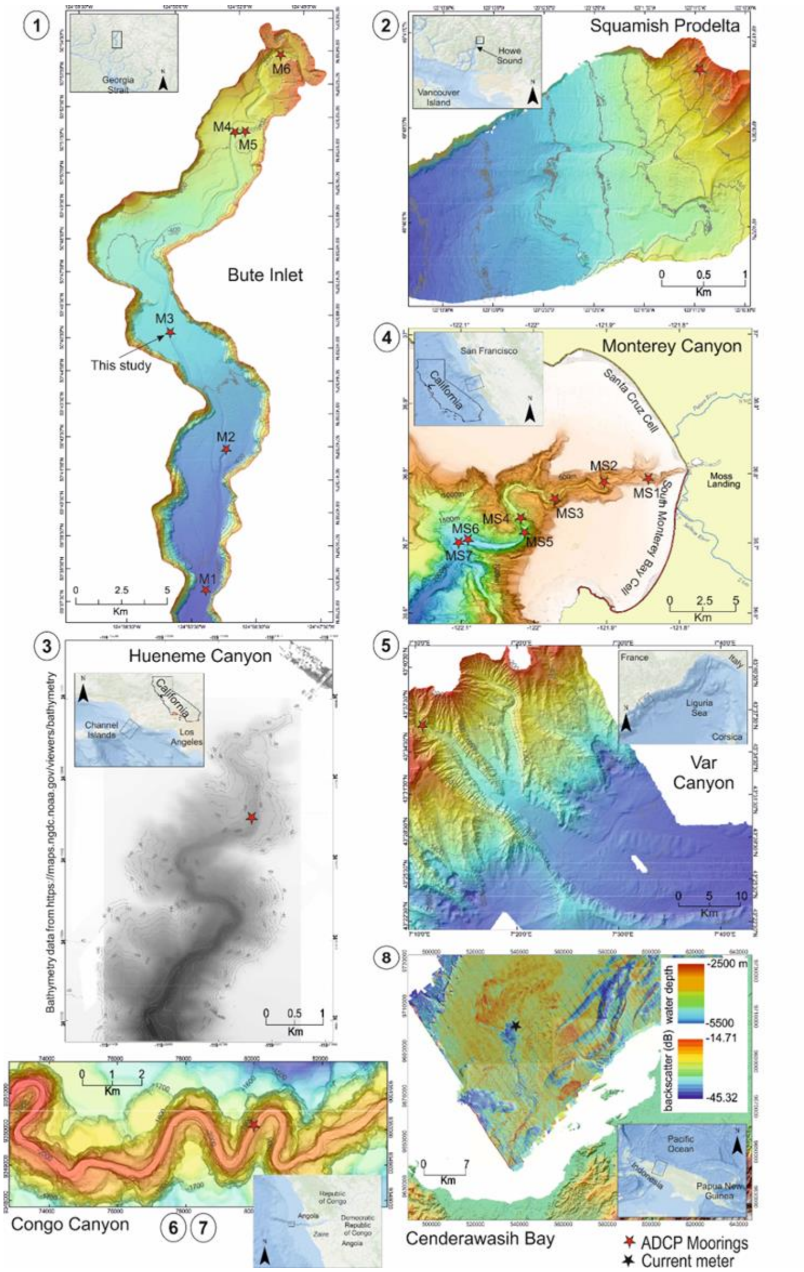

Figure S1. location map of the sites where turbidity currents have been monitored in action and analyzed in our study. Bute Inlet and Squamish Delta (British Columbia) are representative of fjord-head systems. Hueneme and Monterey canyons (California), represent littoral drift-fed submarine systems. Var canyon (south Mediterranean Sea), Congo canyon (offshore Angola) and Cenderawasih Bay (West Papua New Guinea) are representative of deep-sea submarine systems directly linked to the rivers activity (see Table S1 & S2 of the supporting material for the reference relative to each area).

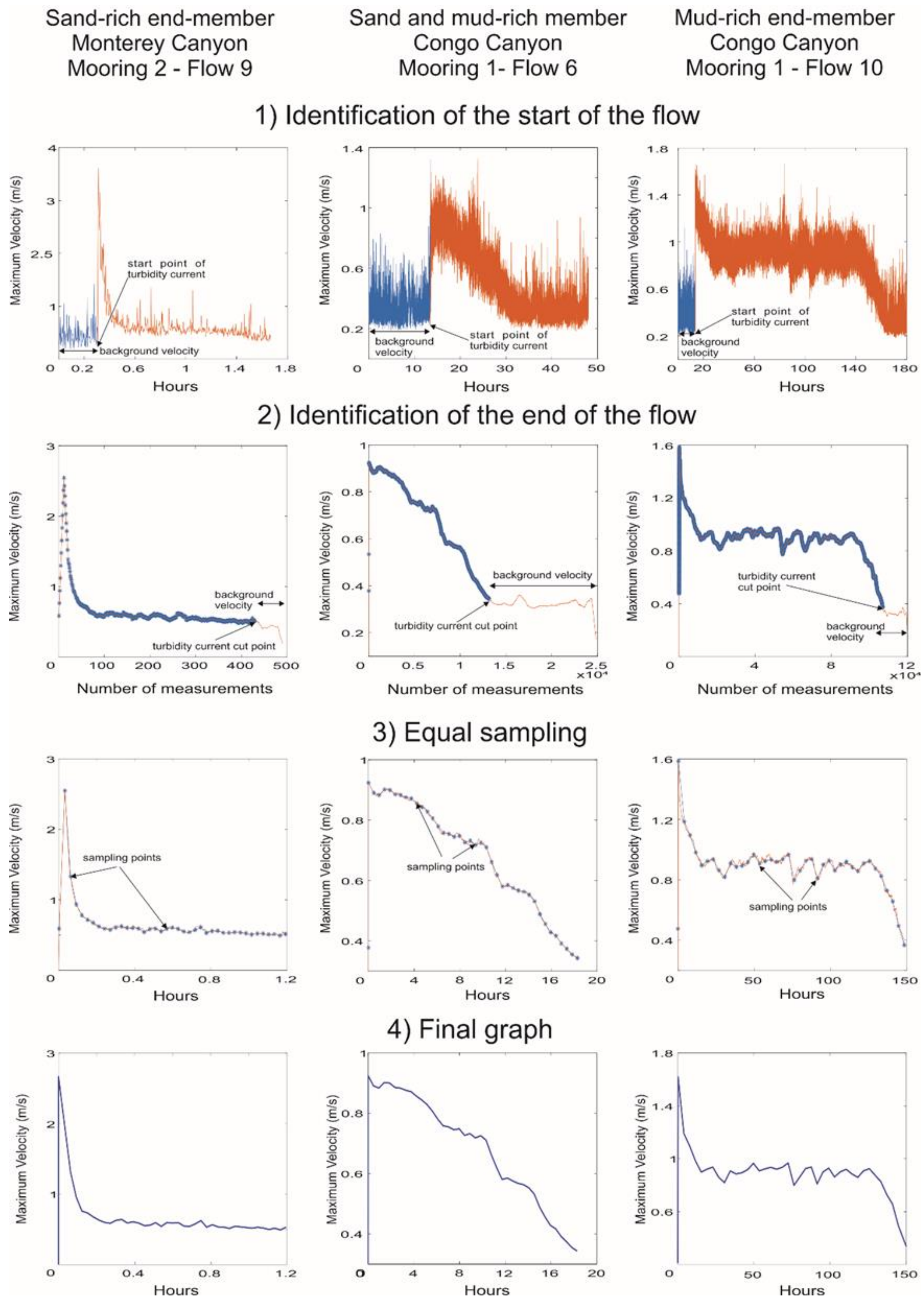

Figure S2: schematic illustration of the methodology developed and applied to identify the of turbidity currents analyzed in this study. Events, ultimately, are plotted as graphs of time versus maximum velocity. Refer to the main text for the specification of our methods.

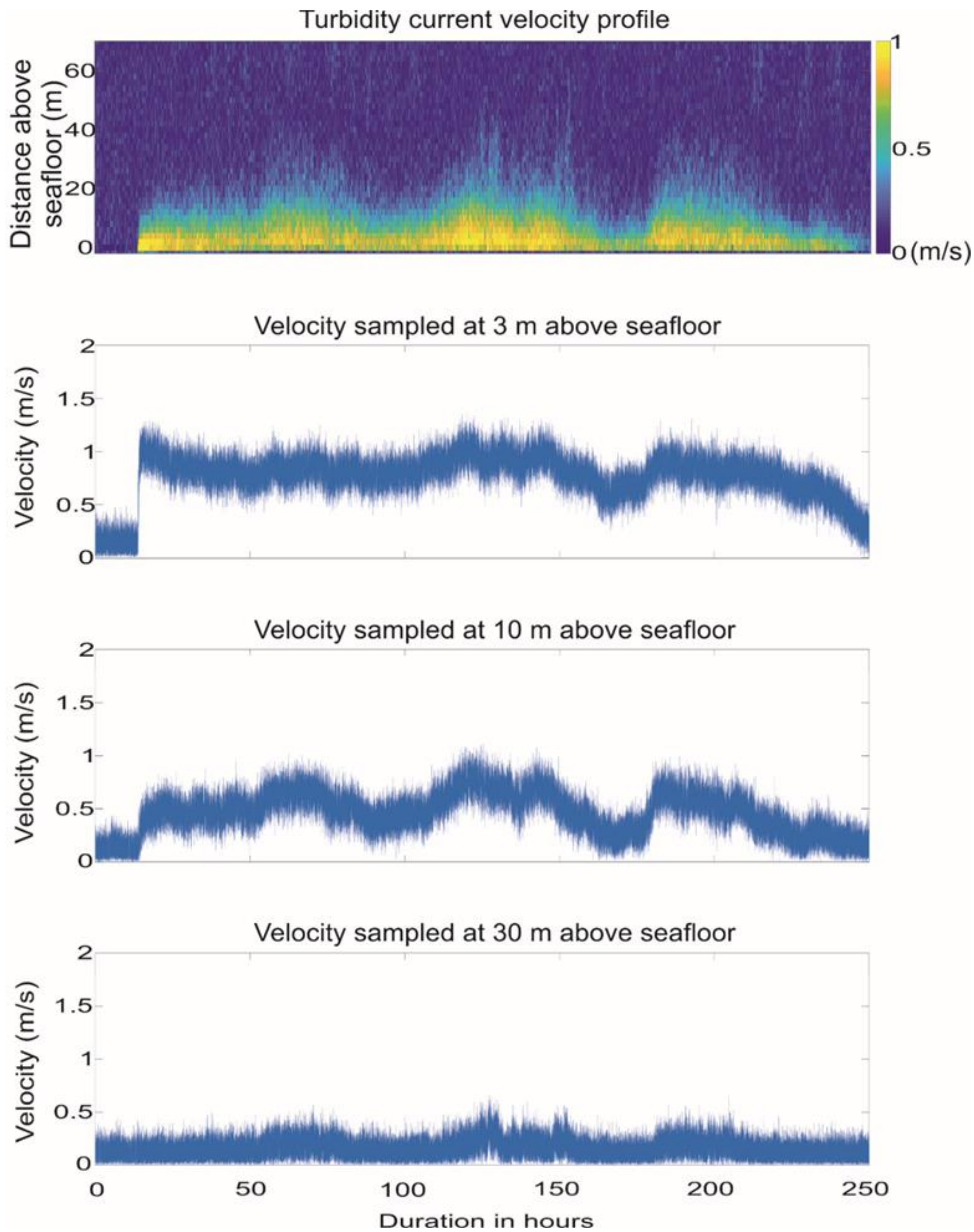

Figure S3: example of velocity profiles extracted at different heights of the water column and relative to Flow 01 of Congo Canyon (see Figure 1– Panel 6 in the main text and Table S1 & S2 of the supporting material for the reference to this study)

Systems	Extend of the system	Water depth (m)	Sediments supply	Sediment discharge into the systems	Monitoring data utilized in our study
Congo Canyon	350 km with 3,000 m water depth	2000	River flood/ canyon wall slumping	43 x 10^9 kg yr^{-1} (Bongo-Passi, 1984)	Cooper et al., 20013 & 2016
Var Canyon	16 km within ~2,000 m water depth	130	River flood/ hyperpycnal flow/ canyon wall slumping	1.63 x 10^6 t yr^{-1}	Khripounoff et al., 2012
Hueneme Canyon	10 km within 500 m water depth	184	Littoral drift-fed submarine systems/ hyperpycnal flow	3-6 x 10^6 t yr^{-1}	Xu et al., 2010
Squamish Delta	2 km within 150 m water depth	60	Bed-load dominated fjord-head delta systems	600-700 m^3/s (Hickin, 1989)	Hughes Clarke 2016
Bute Inlet	40 km within 600 m water depth	50	Bed-load dominated fjord-head delta systems	*1.7 × 10^6 to yr^{-1} *amount of sediments delivered to the canyon head (Syvitski et al., 1988)	Hage et al., 2020
Monterey Canyon	153 km within 3,600 m water depth	<2000	Littoral drift-fed submarine systems	300,000 m^3 yr^{-1} (Smith et al., 2005)	Paull et al., 2018.
Cenderawasih Bay	60 km within 1,600 m water depth	<2000	River flood/ hyperpycnal flow	Not known	Wood, 2013

Table S1. Table 1: physical parameters of the physiographic submarine systems analyzed in our study. Water depth is relative to the depth at which the ADCPs were deployed within the water column (See also Table S2)

Grainsize	**Study area**	**Description**	**Reference**
Sand-rich end members	Squamish Prodelta	Structureless sand, poorly graded, with layers of amalgamated sand toward the top.	Hage et al., 2018
	Hueneme Canyon	Fine and very fine sand, to silt and locally lens of clay.	Xu et al., 2010
	Monterey Canyon	Poorly sorted intervals containing coarse gravel or multi-coloured clay clasts near their base, overlain by fining-upward sand with sand-supported rounded cobbles and angular clay chips floating within the sand.	Paull et al., 2010
	Var Canyon	Coarse silt to very fine sand with interbedded thin layers of fine sand.	Klauche et al., 2000
Sand and mud- rich members	Bute Inlet	Sand beds, including associated mud top, from 10 cm to 1 m thickness. Mud, including associated mud top and organic debris, interbedded to layers of sand from 10 to 50 cm thickness.	Hage et al., 2019; 2020
	Cenderawasih Bay	Mud and woody organic debris locally interbedded by very thin layers of sand.	Orange et al., 2010
Mud-rich end members	Congo Canyon	Mud locally interbedded by very thin layers of sand. Often present laminations typically plane-paralled, in some cases, sub-parallel.	Azpiroz-Zabala et al., 2017

Table S3. Table S3: lithological characterization of the core logs represented in Figure 2 - Panel C in the main text.